Available online at www.sciencedirect.com

ScienceDirect

Proceedings of the Combustion Institute 36 (2017) 4443–4451

Proceedings of the Combustion Institute

www.elsevier.com/locate/proci

Tailor-making thermocouple junction for flame temperature measurement via dynamic transient method

Zuwei Xu, Xin Tian, Haibo Zhao*

State Key Laboratory of Coal Combustion, School of Energy and Power Engineering, Huazhong University of Science and Technology, PR China

Received 3 December 2015; accepted 24 August 2016
Available online 5 October 2016

Abstract

Traditional dynamic method for temperature measurement is generally based on the assumption that the thermal inertia coefficient of a thermocouple junction is invariable (time constant) within the whole measuring process. Furthermore, the effect of heat conduction and heat radiation on the temperature response of the thermocouple is simply neglected under certain conditions. In this study, a new concept is proposed for improvement of the traditional dynamic method. The key point of the newly-proposed method is to tailor-make a thermocouple junction diameter to realize accurate compensation for radiation heat loss and specific heat capacity rising with the heat conduction from wires to the junction, which eventually makes the temperature response curve of the thermocouple still comply with the first-order response equation. The proposed method can be used for temperature measurement of high temperature flame, fine particle-laden flame as well as lab-scale small flame. Heat sink at the thermocouple junction due to heat conduction from neighboring wires to the junction is observed via numerical calculation, which can compensate the temperature rise lag of the junction caused by the radiation heat loss and the increase of specific heat capacity. Thus, there is no need to neglect the effect of heat conduction, heat radiation and thermal inertia coefficient variation on temperature measurement as in the traditional dynamic method. A thermocouple with the junction diameter of 0.7 mm can retain relatively long time (*ca.* 2 s) of steady apparent thermal inertia coefficient. The tailor-made thermocouple is applied to measure the temperature of TiO_2 aerosol flame and sooting flame. The temperature measurement results agree well with both simulation results and benchmark experimental results, which indicates that the improved dynamic method and the tailor-made thermocouple can be employed to measure the temperature of fine particle-laden flame in a relatively straightforward manner.

Keywords: Thermocouple; Junction design; Flame temperature measurement; Heat conduction compensation; Thermal inertia coefficient

1. Introduction

A fine-wire thermocouple is widely used in flame temperature measurement, which transfers thermal signal into electric potential signal, easy for signal

* Corresponding author. Fax: +86 27 8754 5526.
E-mail address: hzhao@mail.hust.edu.cn (H. Zhao).

http://dx.doi.org/10.1016/j.proci.2016.08.071
1540-7489 © 2016 by The Combustion Institute. Published by Elsevier Inc.

remote transmission and conversion. Moreover, it has the merits of simple structure, high reliability and cost efficiency. Generally, for temperature measurement of an optically thin flame, the unsteady energy differential equation of the thermocouple junction can be written as [1]

$$\frac{\partial T}{\partial t}=a\frac{\partial^2 T}{\partial x^2}+\frac{h(T_g-T)}{\rho c}\frac{\mathrm{d}A}{\mathrm{d}V}+\frac{\varepsilon\sigma}{\rho c}(T_\infty{}^4-T^4)\frac{\mathrm{d}A}{\mathrm{d}V} \tag{1}$$

where the three terms on the right side represent heat conduction along the wire, heat convection between the thermocouple and the flame, heat radiation between the thermocouple and surrounding, respectively. In Eq. (1), T, T_g and T_∞ represent the thermocouple junction temperature, the actual flame temperature and the surrounding temperature, respectively; a is the thermal diffusion coefficient of the thermocouple, $a = \lambda/(\rho c)$, λ, ρ and c are the thermal conductivity, density and specific heat capacity of the thermocouple material (wire and junction), respectively; h is the convective heat transfer coefficient; $\mathrm{d}A$ and $\mathrm{d}V$ represent the heat exchange area element and thermocouple volume element, respectively; ε is the emissivity; σ is the Stefan-Boltzmann constant (5.67×10^{-8} W m^{-2} K^{-4}). Generally, the application of a thermocouple in temperature measurement varies in steady-state method, quasi-steady-state method and dynamic transient method.

Steady-state method is a means to achieve or approximately approach thermal equilibrium (*i.e.* $\partial T/\partial t = 0$) among the thermocouple, measured object and surrounding with a relatively long exposure time in flame. Due to the melting point limitation of thermocouple material, the steady-state method is not suitable for very high temperature measurement. Besides, the temperature of the thermocouple junction will be affected by heat conduction along the thermocouple wire, radiation heating or radiation heat loss, which eventually leads to significant measurement error. The thermocouple measurement errors are to be corrected which otherwise would lead to serious deviation in measured temperature value from the actual value. At present, there are mainly two correction methodologies available in literature: instrumental correction method and numerical correction method. In the first method, aspirated thermocouple [2], rotated thermocouple [3], two-thermocouple (two junctions of different diameters) [4] or multi-thermocouple (multiple junctions of different diameters) [5] were used to measure the flame temperature. For the aspirated thermocouple and rotated thermocouple, radiation-derived measurement error was reduced by enhancing heat convection around the bead; while the two or multi-thermocouple was based on the hypothesis that radiation loss is negligible for a zero dimension diameter wire, and temperature at zero diameter could be obtained by extrapolating the measured temperature at different wire diameters. However, the conduction losses were not corrected in the first method. Conduction error is significant especially for larger wire diameters and shorter lead wire lengths as demonstrated by Bradley and Matthews [6]. Numerical correction method computes the conduction error as well and is therefore the more appropriate method [7–9]. Generally, multiple empirical formulas with uncertainties that are difficult to quantify were required for the radiation correction method [2,10,11]. Even so, the steady-state method is still impossible for accurate temperature measurement of particle-laden flame or highly sooting flame. It is because the deposition of fine particle on the surface of the thermocouple will constantly change its heat transfer characteristics (such as surface thermal resistance, surface emissivity, junction volume, etc.), resulting in continuously time-varying thermocouple temperature.

The quasi-steady-state method, named as thermocouple particle densitometry (TPD), was first proposed by Eisner and Rosner [12] then improved by McEnally et al. [13] to measure the flame temperature and soot volume fraction simultaneously based on the quasi-steady-state process of thermocouple temperature variation in sooting flame. This diagnostic relies on measuring the junction temperature history of a thermocouple rapidly inserted into a sooting flame, then optimizing the fit between this history and one calculated from the principles of thermophoresis mass transfer [13]. Lu and Zhou [14] considered the enthalpy increment caused by radiation heat transfer of soot particle onto the junction surface and junction temperature change, and improved the energy balance equation in the traditional TPD method. This modification does not require the assumption of particle thermophoretic deposition any more. However, due to the complex influence of particle deposition on thermocouple heat transfer, some simplified treatments and numerical computation were required in practical application, which eventually makes inconvenient operation and insufficient accuracy for the TPD method.

With respect to the dynamic transient method, the thermocouple probe is rapidly inserted into the flame, and the temperature response curve of the thermocouple is recorded. Due to relatively short residence time in flame, the temperature of the thermocouple junction can be considerably low when compared with the actual flame temperature, and then the radiation loss can also be ignored. On the other side, if the thermocouple with a relatively long wire is inserted deeply into the flame, the heat conduction loss (for junction diameter as same as wire diameter) of the junction along the wire can also be neglected. When the dominant mechanism of heat transfer is pure convection, the non-steady heat transfer Eq. (1) of the thermocouple is

simplified as

$$\frac{dT}{dt} = \frac{hA(T_g - T)}{\rho cV} \quad (2)$$

Define the thermal inertia coefficient of the thermocouple junction

$$\tau = \frac{\rho cV}{hA} \quad (3)$$

If c and h remain constant, τ can be regarded as the time constant of the thermocouple junction. With the initial thermocouple temperature T_0 at time t=0, the solution of Eq. (2) conforms to the first-order response equation [15]

$$T = T_g - (T_g - T_0)e^{-t/\tau} \quad (4)$$

The flame temperature T_g and τ can be obtained by using the least square method with the first-order equation to fit the temperature response curve of the thermocouple.

The temperature measuring range of the dynamic transient method is not limited by the melting point of thermocouple material any more. This method can measure flame of 2000–3500 °C and even much higher in, *e.g.*, rocket engines and jet engines [16]. Moreover, the quite short exposure duration of the thermocouple in flame can significantly reduce particle deposition on the thermocouple surface, therefore the dynamic transient method has obvious superiority on measuring particle-laden flame [17]. However, as the thermo-physical properties of the thermocouple (particularly, the specific heat capacity of the thermocouple) vary a lot with temperatures, the assumption of constant thermal inertia coefficient will bring significant calculation error [18]. Chen et al. [18] corrected the thermal inertia coefficient τ as the function of temperature T, $\tau=\tau_0(1+\alpha T)$, according to the relationship of T and specific heat capacity c of the thermocouple ($c=c_0(1+\alpha T)$), where c_0 and τ_0 represent the specific heat capacity and thermal inertia coefficient of the thermocouple at 0 °C, respectively; α is the temperature constant; T is with dimension of °C here. On the other side, it is noted that the heat conduction along the thermocouple wire should not be neglected if the thermocouple wire inserting the flame is short or the gas velocity is relatively low, and radiation loss is also not negligible when the heat convection is not very intense. This situation usually appears in laboratory-scale small flames. From this perspective, numerical calculation is required for inversion of the flame temperature, which greatly increases the complexity of the temperature measurement process.

Factually, since the junction diameter is usually larger than the wire diamater, the thermal inertia of the junction is also larger than that of the wire. Consequently, the temperature rising rate of the wire near the junction is faster than that of the junction during the dynamic response. It means that the wire temperature around the junction is higher than that of the junction, which contributes to heat conduction from thermocouple wires to the junction. This eventually results in a heat sink formed in the thermocouple. If the heat conduction into the junction can perfectly offset the radiation loss out the junction and the effect of the temperature lag caused by the increase of specific heat capacity, it is possible that the temperature evolution of the junction satisfies the first-order response equation without ignoring the heat conduction and radiation loss as in the conventional dynamic transient method. In such a way, a simple numerical fitting to the first-order response curve is available for flame temperature inversion, which exhibits the advantages of simplified data analyzing and improved measurement precision. The objective of this work is to tailor-make the junction diameter (which influences the heat conduction most significantly) to attain perfect "balance compensation" among heat conduction inwards, radiation loss outwards and increasing specific heat capacity of materials so as to achieve the first-order response within sufficient time. Numerical calculation is conducted to investigate the effect of thermocouple junction diameter on temperature response characteristic of a B-type thermocouple. The optimal junction diameter and exposure duration of the thermocouple in flame are determined, and the temperature profiles of two typical flames, one TiO_2 aerosol flame and another highly sooting flame, are measured by the tailor-made thermocouple based on the improved dynamic transient method. The experimental measurements are compared with numerical results or available benchmarkdata.

2. Numerical calculations and analysis for the design of junction diameter

2.1. Dynamic heat transfer of a thermocouple

The investigated object is a B-type fine-wire thermocouple (PtRh30 (70 wt% Pt/30 wt% Rh as positive wire) - PtRh6 (94 wt% Pt/6 wt% Rh as negative wire), Omega Engineering), and the diameter of both lead wires is d=0.3 mm. While for the junction (with the shape of a spherical segment that can be described as a melt-bonding bead amputating the lead wires), eight different diameters (D) are considered, *i.e.*, 0.3, 0.4, 0.5, 0.6, 0.7, 0.8, 0.9, 1.0 mm. The length of the positive and negative wires are both 50 mm, and the thermocouple junction is located in the middle of two alumina insulating tubes, as shown in Fig. S1 of the supplemental material (SM). Assuming that a representative homogenous and cylindrical flame is vertical upward with a diameter of 20 mm, the gas composition contains H_2O, CO_2 and Ar (with the mole ratio of 2:1:1), the gas flow velocity is u_g=1 m/s and the flame temperature is T_g=1800 K. The thermocouple is horizontally inserted into the flame for

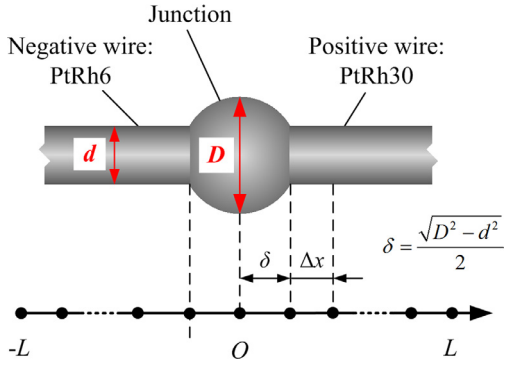

Fig. 1. One-dimensional grid representation of wire and junction of the thermocouple.

temperature measurement and the junction is located at the flame axis. Setting the junction center as the origin of coordinate and the positive wire as the positive half axis, the one-dimensional grid along the two wire directions (with total length of $2L$=100 mm) is uniform, with the grid spacing Δx=0.5 mm, as shown in Fig. 1.

The finite difference method is employed to solve Eq. (1) of the thermocouple, in which both convection and radiation are regarded as source terms. The explicit difference form of Eq. (1) at ith grid and kth time step can be written as

$$\frac{T_{i,k+1} - T_{i,k}}{\Delta t} = a\frac{T_{i+1,k} - 2T_{i,k} + T_{i-1,k}}{(\Delta x)^2} + S(x_i, t_k) \tag{5}$$

in which, source terms read

$$S(x_i, t_k) = \begin{cases} \dfrac{h(T_g - T_{i,k})}{\rho c}\dfrac{dA}{dV} + \dfrac{\varepsilon\sigma}{\rho c}(T_\infty^4 - T_{i,k}^4)\dfrac{dA}{dV}, \\ -10 \le x \le 10 \\ \dfrac{h(T_\infty - T_{i,k})}{\rho c}\dfrac{dA}{dV} + \dfrac{\varepsilon\sigma}{\rho c}(T_\infty^4 - T_{i,k}^4)\dfrac{dA}{dV}, \\ -50 < x < -10,\ 10 < x < 50 \end{cases} \tag{6}$$

where Δt is time step.

For spherical junction, the dimensionless heat transfer coefficient and the ratio of heat exchange area and volume can be expressed as $\mathrm{Nu} = hl/\lambda_g = 2 + 0.6\mathrm{Re}^{1/2}\mathrm{Pr}^{1/3}$ [8] and $\frac{dA}{dV} = \frac{\pi D^2}{\pi D^3/6} = \frac{12D}{2D^2+d^2}$, respectively. For cylindrical wire, $\mathrm{Nu} = hl/\lambda_g = 0.42\mathrm{Pr}^{1/5} + 0.57\mathrm{Re}^{1/2}\mathrm{Pr}^{1/3}$ [8] is applied to forced convection inside of the flame (within $-10 \le x \le 10$), and $\mathrm{Nu} = hl/\lambda_g = 0.48(\mathrm{Gr}\cdot\mathrm{Pr})^{1/4}$ [19] is applied to natural convection in the air (within $-50 \le x \le -10$ and $10 \le x \le 50$), $\frac{dA}{dV} = \frac{\pi d\Delta x}{\pi d^2\Delta x/4} = \frac{4}{d}$, where l is the characteristic length (for junction bead l=D and for wire l=d), the Reynolds number $\mathrm{Re}=u_g l/\nu_g$, the Prandtl number $\mathrm{Pr}=c_g\nu_g/\lambda_g$, the Grashof number $\mathrm{Gr} = (g\alpha_g\delta_T d^3)/\nu_g^2$, c_g, ρ_g, ν_g, λ_g, and α_g represent the specific heat capacity, density, kinematic viscosity, thermal conductivity coefficient and volume expansion coefficient of gas, respectively. δ_T is the temperature difference between the wire and air. For more details about the thermal physical properties, see Section 2 of SM.

Boundary condition for thermocouple heat transfer calculation is the Dirichlet boundary condition, in which the temperatures at the connection of thermocouple wires and insulating tubes (x=±50 mm) are fixed at 300 K and the initial thermocouple temperature is 300 K, uniformly distributed. To guarantee the stability and convergence of the numerical calculation, the iterative time step is limited to $\Delta t \le (\Delta x)^2/(4a)$, where a is the thermal diffusion coefficient of the thermocouple. Finally Δt is determined as 0.0002 s and the time window is 0–10 s.

The initial thermal inertia coefficient is calculated based on thermal-physical property of the material and heat convection at t=0, $\tau_{\mathrm{initial}} = \frac{\rho c V}{hA}|_{t=0}$. And the apparent thermal inertia coefficient, which characterizes the evolution of thermal inertia coefficient as time t or junction temperature T, is defined as $\tau_a = t/\ln[(T_g - T_0)/(T_g - T)]$.

2.2. Numerical results

Calculations are conducted for eight different junction diameters, D=0.3, 0.4,…,1.0 mm. The junction temperature evolution as a function of time is shown in Fig. 2. The first-order temperature response curves based on the initial thermal inertia coefficient, $T = 1800 - 1500e^{-t/\tau_{\mathrm{initial}}}$, are also shown for comparison (solid lines in Fig. 2). Obviously, all of the calculated junction temperature curves only approach to the first-order response equation within a short time range. Serious deviation occurs when the junction reaching higher temperatures, however the initial deviation temperatures are varied. Among which, the initial deviation temperature of the junction with D=0.7 mm was the highest, nearly 1500 K, and the duration satisfying the first-order response equation was the longest. As seen, the temperature curve of 0.7 mm junction during the first 2 s agrees well with the first-order response curve.

As shown in Fig. 3, all of τ_a remain stable first and then rapidly increase as time. The apparent thermal inertia coefficient of 0.7 mm junction remains the longest stable time, which is 10 times longer than that of other junctions with various diameters.

Figure 4 shows the time-varying temperature profiles of the thermocouples with four typical junction diameters. The temperature of the positive wire (PtRh30) is slightly higher than that of the negative wire (PtRh6). This is because both

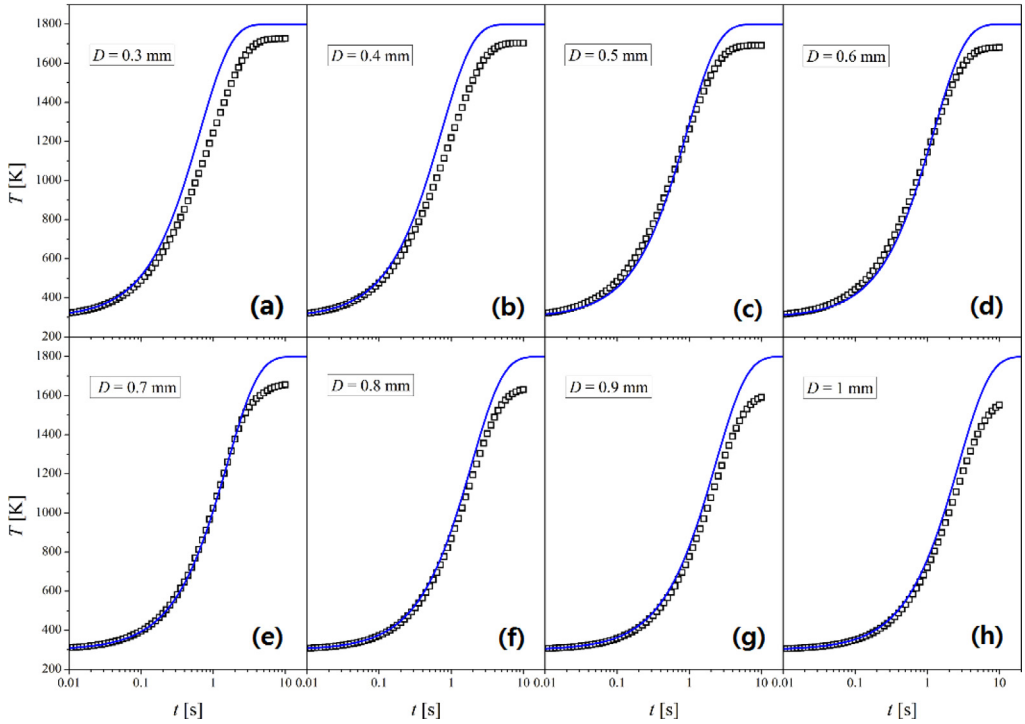

Fig. 2. Temperature response curves of junctions with different diameters (hollow square points) and prediction results by the first-order response equation $T = 1800 - 1500e^{-t/\tau_{initial}}$ (solid lines).

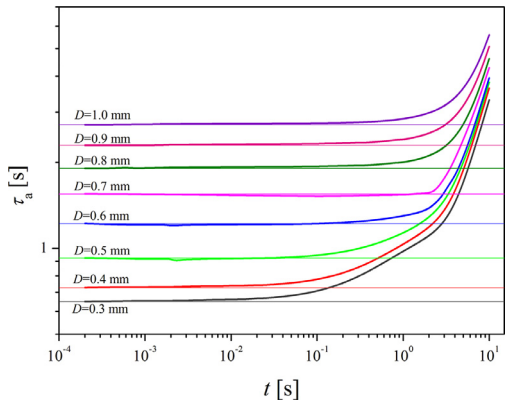

Fig. 3. Evolution of the apparent thermal inertia coefficient of junctions with different diameters as a function of time.

the heat conductivity coefficient and emissivity of PtRh30 are lower than those of PtRh6, resulting in lower heat conduction inwards and radiation loss outwards for the positive wire and then higher temperatures. As seen, when the junction diameter is equal to the wire diameter (D=d=0.3 mm, as shown in Fig. 4a), the temperatures of the junction and neighboring wires increase synchronously with time. However, with the increase of the junction diameter, the temperature difference between the junction and neighboring wires increases gradually. This is because a larger junction diameter having a greater thermal inertia coefficient leads to that the temperature of the junction lags behind that of the neighboring wires. In fact, the heat sink is formed in the thermocouple and heat conduction occurs from wires to the junction. As mentioned above, the junction temperature response is affected by heat conduction, radiation and varying thermal inertia coefficient. If without compensation to thermal inertia coefficient variation and radiation loss by heat conduction inwards, the junction temperature response curve will naturally deviate from the first-order response equation, as seen in Fig. 4a of 0.3 mm junction. For the junctions with diameter of D=0.4 mm and D=1.0 mm, the compensation effect from heat conduction is available, however the heat compensation is not able to perfectly balance the influence of thermal inertia coefficient variation and radiation loss because the temperature gradient between the junction and neighboring wires is relatively small for 0.4 mm junction (Fig. 4b) or the specific heat capacity of 1.0 mm junction was quite large (Fig. 4d). Instead, the most appropriate "balance compensation" for the 0.7 mm junction (Fig. 4c) makes the junction tem-

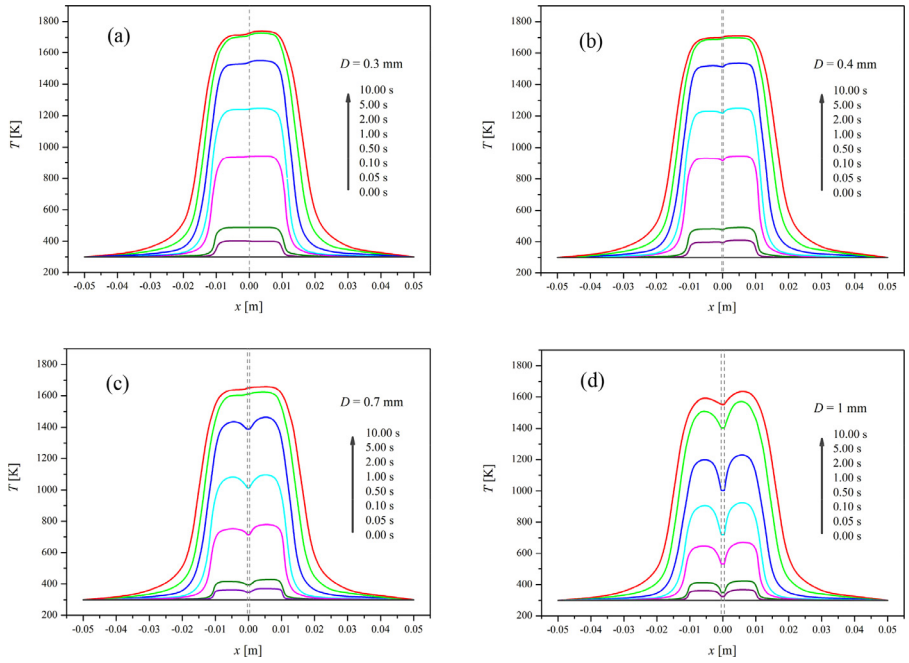

Fig. 4. Time-varying temperature profiles of thermocouples with four typical junction diameters.

Table 1
The increase ratio of integrative heat transfer coefficient and specific heat capacity for typical junction diameters.

t [s]		0.05	0.10	0.50	1.00	2.00	5.00	10.00
D=0.3 mm	η	−0.012	−0.031	−0.046	−0.116	−0.218	−0.362	−0.558
	χ	0.031	0.052	0.161	0.233	0.305	0.347	0.350
D=0.4 mm	η	0.009	0.026	−0.035	−0.122	−0.175	−0.313	−0.467
	χ	0.029	0.049	0.155	0.228	0.298	0.342	0.344
D=0.7 mm	η	0.017	0.029	0.106	0.215	0.268	0.015	-0.121
	χ	0.018	0.029	0.106	0.216	0.269	0.322	0.332
D=1.0 mm	η	0.008	0.010	0.034	0.081	0.132	0.257	0.183
	χ	0.013	0.019	0.062	0.108	0.176	0.272	0.308

perature response curve comply with the first-order response equation.

The integrative heat transfer coefficient between junction and flame is defined as $h_i=(q_{Cond}+q_{Rad}+q_{Conv})/(T_g-T)$, where q_{Cond}, q_{Rad} and q_{Conv} are the conduction, radiation and convection heat fluxes of junction, respectively. The increase ratio of h_i and c (specific heat capacity) are respectively defined as $\eta=(h_i-h_{i0})/h_{i0}$ and $\chi=(c-c_0)/c_0$, where the subscript 0 denotes initial state. As shown in Table 1, for the 0.7 mm junction, η can keep pace with χ during the first 2 s, whereas other three junctions fail to maintain the synchronization relationship. Therefore, the thermal inertia coefficient of 0.7 mm junction is invariable within 0–2 s according to Eq. (3).

For the temperature response curve obtained by the thermocouple with junction diameter D=0.7 mm within 0–2 s, the function $y=P_1+P_2\exp(-x/P_3)$ is employed for nonlinear fitting, as shown in Fig. 5. Three parameters, P_1=1743.7, P_2=1445.2 and P_3=1.518, are attained, where P_1 is the flame temperature, (P_1–P_2) represents the initial temperature of the thermocouple and P_3 is the time constant. When compared P_1, (P_1–P_2) and P_3 with known flame temperature 1800 K, initial temperature 300 K and initial time constant 1.549 s, the relative deviations are only 3.13%, 0.5% and 2%, respectively.

Therefore, the diameter of the B-type thermocouple junction is optimized as 0.7 mm. For the investigated flame with a temperature of 1800 K and gas velocity of 1 m/s, the time constant is about 1.5 s and it can keep stable within 0–2 s (see Fig. 3). The time constant and stable response interval are also appropriate for temperature measurement of particle-laden flame, which can not only guarantee sufficient response signal but also reduce

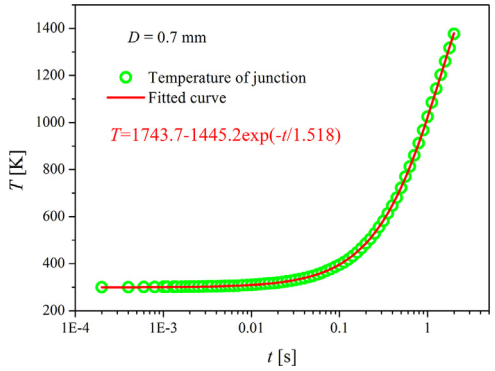

Fig. 5. Temperature response of the optimized junction (D=0.7 mm) and the fitting curve within the time range of 0–2 s.

the adverse effect of particle deposition on the thermocouple. Some uncertainties are associated with the temperature response fitting of the optimized junction (D=0.7 mm), particularly with the ambient temperature (T_∞) and gas composition variations. An analysis about uncertainties of the numerical optimization is provided in Section 4 of SM. In general, when the ambient temperature is less than 400 K, the relative error is limited to 5%; the effect of gas composition variation on the temperature measurement is not obvious (uncertainty below 4%).

3. Experimental

3.1. Nanoparticle-laden flame

In order to verify the temperature measurement accuracy of the improved dynamic transient method, two typical particle-laden flames, a TiO_2-laden flame and a sooting flame, are measured using the tailor-made thermocouple (d=0.3 mm and D=0.7 mm).

For the TiO_2-laden flame, a co-flow diffusion burner is designed, and four concentric tubes are aerated with $TiCl_4$ vapor carried by N_2, CH_4+Ar (fuel), O_2 (oxidizer) and N_2 (sheath gas) from the center to the outside [17]. The gas flow rate of CH_4/Ar mixture is 1.80 NL/min, in which the methane flow rate contributes to 1.20 NL/min. The vaporizer temperature of precursor $TiCl_4$ is 65 °C, with the pressure of 1 atm. The nanoparticles TiO_2 are formed by the oxidation of $TiCl_4$ vapor at production rates of 14.4 g/h. Three different O_2 flow rates are designed in this work, as Case A-2.40 NL/min, Case B-2.88 NL/min and Case C-3.60 NL/min, in which the O_2 flow rate of Case A is calculated based on the stoichiometric ratio for complete combustion of methane. The excess oxygen coefficients for Case B and Case C are 1.2 and 1.5, respectively. Eleven different axial heights of the flame (HAB, with the burner outlet as the starting point), T1-T11 (HAB=5, 15, 25, 35, 45, 55, 65, 75, 85, 95, 105 mm), are selected as temperature measurement points. More details on the laboratory apparatus for the synthesis of TiO_2 nanoparticle and experimental conditions can be found in Section 1 of SM.

The axial temperature profiles are measured by the tailor-made thermocouple. The residence time of the thermocouple in flame is 2 s, controlled by the timer function of the PLC (programmable logic controller). The thermocouple is rapidly swept into the intended sampling position in the flame by the three-axis translation stage (the translational speed is approximately 0.5 m/s), before being removed after two seconds. The travel time (approximately 0.02 s) is about 1% of the residence time, minimizing the disturbance to flame. The signal acquisition frequency of the thermocouple is 50 Hz, *i.e.*, recording a data point (T, t) every 0.02 s. Generally, data is acquired a few seconds before the thermocouple enters into the flame and stopped after the thermocouple is removed out of the flame. Thus, the obtained (T, t) data should be treated to determine the non-linear fitting starting point of the first-order response equation as well as the effective fitting interval, detailed in Section 3 of SM.

Once the non-linear fitting starting point and effective interval are determined, the junction temperature response curves recorded (as shown in Fig. S5(a), (b), (c)) are used to obtain flame temperature (P_1), initial temperature (P_1-P_2) and thermocouple time constant (P_3) via fitting these to the first-order response function $T=P_1+P_2\exp(-t/P_3)$. Nonlinear least square fitting (NLSF) is employed in this work and fitting factor R^2 is over 0.999 for all the curves. Excellent fitting result is obtained, with the error for P_1 in the range of ±5.0 °C and the error for P_3 in the range of ±0.02 s. The thermocouple time constant at different sampling points is shown in Fig. S5(d). As seen, the time constant slightly fluctuates around 1.5 s with the range of ±0.06 s and the relative deviation to the initial thermal inertia coefficient is about 4%.

The experimental measurements are compared with the computational fluid dynamics (CFD) simulation results. The flame model consists of the continuity equation, the Navier–Stokes (N–S) equations for momentum, the k-ε turbulence equations, the species transport equations based on the eddy dissipation model (EDM) and the radiation transport equation. The reaction rate of methane and oxygen combustion in the diffusion flame is approximated by a single-step reaction with an Arrhenius expression. Radiation is taken into account by the P-1 model, and a composition-dependent absorption coefficient for CO_2 and H_2O mixtures is defined using the weighted sum of gray gases model (WSGGM) (Fluent 6.3 User's Guide). The computation is implemented in the commercial

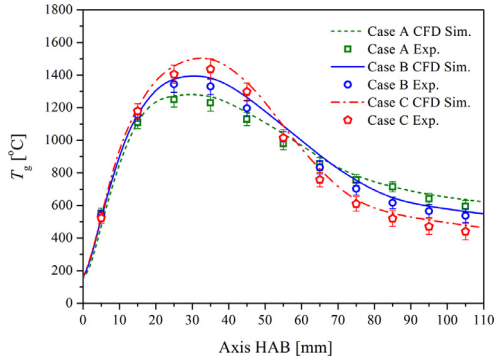

Fig. 6. Axial temperature profiles measured and simulated for three cases in TiO_2-laden flame, where the measurement error bar is obtained by five repeated measurements.

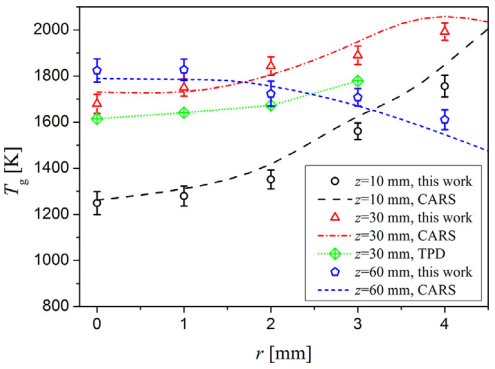

Fig. 7. Comparisons of temperature measurements in a benchmark sooting flame.

CFD software Fluent. Section 5 in SM provides more details on numerical model and methods of the flame simulation.

The temperature profiles along the axial height of the flame for three cases are shown in Fig. 6. The flame temperature first increases rapidly with the increase of the axial height, then decreases slowly after a peak temperature is achieved. Generally, the experimental measurements for the temperature field, the evolution trend, the maximum temperature and its position agree quite well with the numerical results. However, the simulated temperatures are generally higher than the measured ones, especially in the high-temperature section (*ca.* 15–45 mm of HAB). These deviations may arise from high-temperature enhancing radiation between the thermocouple and the surrounding as well as between TiO_2 particles and the surrounding. Another explanation is the temperatures predicted by the Fluent simulations typically contain model uncertainties and calculation errors.

3.2. Sooting flame

The experiment is conducted in an ethylene/air laminar diffusion flame, in which the burner is same as that reported by National Research Council Canada [20]. The detailed description of the Gülder burner can be found in [21]. A representative benchmark condition is employed in our sooting flame measurements, in which the flame is generated with ethylene and air flow rates of 0.194 NL/min and 284 NL/min respectively, as shown in Fig. S3.

In this work, we measure the radial temperatures (*i.e.,* r=0, 1, 2, 3, 4 mm) at three HABs (z=10, 30, 60 mm) and then attain two-dimensional temperature profiles of the sooting flame by the dynamic transient method, using the same thermocouple and same measurement procedure in the TiO_2-laden flame. The results are compared with a benchmark experiment by coherent anti-Stokes Raman scattering (CARS) thermometry [20], as shown in Fig. 7. It can be found that the results obtained from the dynamic transient measurement agree well with the laser-based method. The relative deviation is smaller than 6%. Furthermore, error bars of five repeated measurements indicate that the precision of the dynamic transient method can be limited within ±50 K. A discussion of experimental uncertainties is presented in Section 4 of SM. When considering, particle deposition, optically thin flame assumption and catalytic effects on the thermocouple surface, the net temperature measurement uncertainty is about ±5%.

Moreover, the thermocouple particle densitometry (TPD) method is employed to corroborate the dynamic transient method, in which a B-type thermocouple is same as the design presented by McEnally et al. [13] with wire diameter of 0.075 mm and bead diameter of 0.3 mm. As seen in Fig. 7, the gas temperature is significantly undervalued because the TPD method inherently relies on the empirical parameters of soot aggregates (*e.g.,* the density) and neglects the heat conduction of wires. For this reason, the dynamic transient method with the tailor-made thermocouple is vital to improve the accuracy and robustness of thermocouple thermometry.

4. Conclusions

A new way is proposed in this work for improving the traditional dynamic method of temperature measurement. The tailor-made thermocouple is able to realize accurate compensation for radiation heat loss and thermal inertia coefficient variation with the heat conduction from the wires to the junction, which eventually makes the temperature response curve of the thermocouple still comply with the first-order response equation. From this perspective, there is a simple and direct approach

to characterize the effects of heat conduction, heat radiation and thermal inertia coefficient variation on temperature measurement, which are usually neglected in the traditional dynamic method. It is clear from numerical calculation that there exists heat sink at the thermocouple junction by heat conduction from neighboring wires to the junction, which can compensate the temperature lag of the junction caused by the radiation heat loss and the increase of specific heat capacity. The tailor-made thermocouple with the junction diameter of 0.7 mm can retain relatively long time (about 2 s) of invariable apparent thermal inertia coefficient and is applied to measure the temperature of TiO_2-laden flame and sooting flame. The measurement results agree well with both simulation results and benchmark experimental results. For different occasions on combustion and flame, appropriate dimensions of thermocouples can be rationally designed via the simple preliminary numerical calculation, and consequently the accuracy and robustness of thermocouple thermometry will be effectively improved in nature.

Acknowledgments

This research was funded by National Natural Science Foundation of China (Grant Nos. 51276077, 51390494, 51606079 and 51522603) and China Postdoctoral Science Foundation (Grant No. 2016M592331).

Supplementary materials

Supplementary material associated with this article can be found, in the online version, at doi: 10.1016/j.proci.2016.08.071.

References

[1] I. Aksit, J. Moss, *Fuel* 84 (2005) 239–245.
[2] L.G. Blevins, W.M. Pitts, *Fire Saf. J.* 33 (1999) 239–259.
[3] S. Krishnan, B.M. Kumfer, W. Wu, J. Li, A. Nehorai, R.L. Axelbaum, *Energy Fuels* 29 (2015) 3446–3455.
[4] S. Brohez, C. Delvosalle, G. Marlair, *Fire Saf. J.* 39 (2004) 399–411.
[5] D.S. De, *J. Inst. Energy* 54 (1981) 113.
[6] D. Bradley, K.J. Matthews, *J. Mech. Eng. Sci.* 10 (1968) 299–305.
[7] D. Collis, M. Williams, *J. Fluid Mech.* 6 (1959) 357–384.
[8] V. Hindasageri, R.P. Vedula, S.V. Prabhu, *Rev. Sci. Instrum.* 84 (2013) 024902.
[9] M. Saffaripour, A. Veshkini, M. Kholghy, M.J. Thomson, *Combust. Flame* 161 (2014) 848–863.
[10] M. Heitor, A. Moreira, *Prog. Energy Combust. Sci.* 19 (1993) 259–278.
[11] N. Bahlawane, U. Struckmeier, T.S. Kasper, P. Oßwald, *Rev. Sci. Instrum.* 78 (2007) 013905.
[12] A.D. Eisner, D.E. Rosner, *Combust. Flame* 61 (1985) 153–166.
[13] C.S. McEnally, Ü.Ö. Köylü, L.D. Pfefferle, D.E. Rosner, *Combust. Flame* 109 (1997) 701–720.
[14] J. Lu, H. Zhou, *J. B. Inst. Technol.* 18 (2009) 402–407.
[15] M. Tagawa, T. Shimoji, Y. Ohta, *Rev. Sci. Instrum.* 69 (1998) 3370–3378.
[16] Q. Xu, *Meas. Sci. Technol.* 14 (2003) 1381.
[17] Z. Xu, H. Zhao, *Combust. Flame* 162 (2015) 2200–2213.
[18] X. Chen, *J. Funct. Mater.* 10 (1979) 16–27.
[19] V.T. Morgan, The overall convective heat transfer from smooth circular cylinders, in: F.I. Thomas, P.H. James (Eds.), Advances in Heat Transfer, Elsevier, 1975, pp. 199–264.
[20] F. Liu, H. Guo, G.J. Smallwood, Ö.L. Gülder, *J. Quant. Spectrosc. Radiat. Transf.* 73 (2002) 409–421.
[21] D.R. Snelling, K.A. Thomson, G.J. Smallwood, Ö.L. Gülder, E.J. Weckman, R.A. Fraser, *AIAA J.* 40 (2002) 1789–1795.